Analytical solution of four-mode coupling in shear strain loaded fiber Bragg grating sensors

Mathias S. Müller,* Hala J. El-Khozondar, Thorbjörn C. Buck, and Alexander W. Koch

Institute for Measurement Systems and Sensor Technology, Technische Universität München, Theresienstrasse 90/N5, 80333 Munich, Germany
Corresponding author: m.s.mueller@tum.de

The polarization-dependant reflection spectra of fiber Bragg grating (FBG) sensors in polarization-maintaining fibers are influenced by shear strain. This influence can be evaluated from a tensorial coupled-mode theory approach. Yet, this approach requires the numerical integration of the four coupled-mode equations. We present an easy to handle, completely analytical treatment of the polarization-dependent reflection spectra of FBGs. We derive the required equations and compare the results to the numerical integration of the four tensorial coupled mode equations. © 2009 Optical Society of America

OCIS codes: 060.0060, 060.2370, 060.2300, 060.2420.

Fiber Bragg gratings (FBG) are currently being investigated for their employment as multiparameter strain sensors [1–5]. FBGs written into polarization-maintaining fibers (PMFs) exhibit two narrow reflection peaks at the Bragg wavelengths $\lambda_{B,p}$ and $\lambda_{B,s}$ corresponding to the two modes of polarization, p and s. These modes possess two different effective refractive indices $n_{e,p/s}$ yielding the two differing Bragg wavelengths from the Bragg condition $\lambda_{B,i} = 2n_{e,i}\Lambda$, where Λ is the grating period. Both $n_{e,i}$ and Λ are functions of the strain applied to the fiber at the position of the FBG, represented by the strain tensor $\bar{e}$. It has been suggested to add a second FBG at the same position but at a strongly different wavelength such that four individual parameters can be extracted from the FBG's position. Then the principal strains, i.e., the diagonal entries of the strain tensor and the temperature, can be reconstructed [6]. A requirement is that the influence of the off-diagonal strain tensor entries, namely the shear strains, on the spectral response of the FBG are negligible.

However, these shear strains, explicitly the e_{xy} component, do influence the spectral response, as we recently pointed out [7,8]. This influence may be calculated by a tensorial coupled-mode analysis, considering the four full guided modes of the polarization-maintaining fiber. The results show that a polarization cross coupling between the modes of orthogonal polarization is induced by the shear strain. This cross coupling is overlapped by the characteristic forward–backward coupling of the grating. As a result, a complicated spectral response of the reflected amplitudes of the two polarization directions can be observed that is strongly distorted with respect to the original, unloaded response. This has implications for the extraction of the measurand, the Bragg wavelengths $\lambda_{B,i}$, and in turn the reconstruction of the diagonal strain tensor entries and the temperature, as we discuss in [9].

The tensorial coupled mode analysis [7] or a transfer matrix method [8] is able to predict the spectral response of the shear strain loaded FBG. However, this prediction can only be conducted by either numerically integrating the coupled-mode equations or numerically performing the transfer matrix approach. Yet, to gain further insight into the problem and possibly derive a solution for it, a manageable analytical solution is required that either approximates the problem well enough or ideally solves it exactly. In this work, we demonstrate how such a solution can be constructed and how it approximates or matches the numerical solution from the tensorial coupled mode analysis. We therefore consider an FBG that is subjected to a strain tensor with shear strains. This situation may arise in an application where the FBG is embedded in a host material. A treatment of shear strains within embedded FBGs has also been given by van Steenkiste and Springer [10], yet this is not applicable to the case in question, since it does not consider the projection of the fundamental modes of the polarization-maintaining measurement fiber onto the perturbed fundamental modes of the shear strain loaded FBG, as will be shown in the following treatment. It is this projection that leads to the observed polarization cross coupling, and therefore to the distortion of the Bragg grating spectra.

The mechanical loading of the host material will result in a strain tensor within the FBG that may, in general, take an arbitrary form. From Pockels law of photoelasticity [11] the change in the impermeability tensor $\bar{\bar{B}}$ upon a load represented by a strain $\bar{e}$ within the fiber may be computed. In a weakly guiding optical fiber only the transversal components of the fields possess a noteworthy amplitude [12], and thus the longitudinal field components are neglected.

From Maxwell's equations a vectorial wave equation may be derived for the transversal field components $\mathbf{D}_t = \{D_x, D_y\}^T$, which for homogeneous media in the direction of propagation takes the form [13]

$$\begin{pmatrix} B_{xx} - n_{e,i}^{-2} & B_{xy} \\ B_{xy} & B_{yy} - n_{e,i}^{-2} \end{pmatrix} \cdot \mathbf{D}_t = \underline{\mathrm{M}}_i \cdot \mathbf{D}_t = 0. \qquad (1)$$

The effective refractive indices of the p- and the s-polarized mode $n_{e,p}$ and $n_{e,s}$ may be found from the

requirement that Eq. (1) possesses a solution and hence the determinant of $\underline{M}_i$ vanishes. Equation (1) only has nontrivial solutions if $\underline{M}_i$ exhibits off diagonal entries, viz. B_{xy} is nonzero and hence the shear strain component e_{xy} is nonzero. Yet, for the case where B_{xy} is zero, the analytical solution of the problem is known [14,15]. The effective refractive indices are thus given by [13]

$$n_{e,p/s}^{-2} = \frac{(B_{xx} + B_{yy}) \pm \sqrt{(B_{xx} - B_{yy})^2 + 4B_{xy}^2}}{2}. \quad (2)$$

We derive the displacement fields of the fundamental modes of the loaded FBG by solving the wave equation (1). This yields for the displacement fields of the p- and s-modes of the loaded fiber

$$\widetilde{\mathbf{D}}_p = \left\{ -\frac{M_{1,12}}{M_{1,11}}, 1 \right\}^T, \quad \widetilde{\mathbf{D}}_s = \left\{ -\frac{M_{2,12}}{M_{2,11}}, 1 \right\}^T, \quad (3)$$

where all variables in the coordinate system of the loaded FBG are indicated by the $\sim$ symbol. To obtain the polarization, we compute the normalized electric fields $\widetilde{\mathbf{E}}_p, \widetilde{\mathbf{E}}_s$ of the modes by

$$\widetilde{\mathbf{E}}_j = \overline{\boldsymbol{B}} \cdot \widetilde{\mathbf{D}}_j / |\overline{\boldsymbol{B}} \cdot \widetilde{\mathbf{D}}_j|. \quad (4)$$

The PMF guiding the light to the FBG is assumed to have its fundamental modes polarized parallel to the coordinate axes x and y (Fig. 1). Thus, the polarization of these fundamental modes can be approximated by $\mathbf{E}_p = \{1, 0, 0\}^T$ and $\mathbf{E}_s = \{0, 1, 0\}^T$. The amplitudes of the four modes in the PMF are labeled $\mathbf{A}_+ = \{A_{p+}, A_{s+}\}^T$ for the forward-propagating modes and $\mathbf{A}_- = \{A_{p-}, A_{s-}\}^T$ for the backward-propagating ones. The amplitudes of the modes inside the FBG are labeled $\widetilde{\mathbf{A}}_j$ accordingly.

We now know the polarization of the modes of the loaded FBG. To find the amplitudes of the fundamental modes of the loaded FBG upon an arbitrary illumination, a projection of the PMF modes onto the FBG modes is required. This projection is found from the continuity requirement of the transversal electric fields, yielding
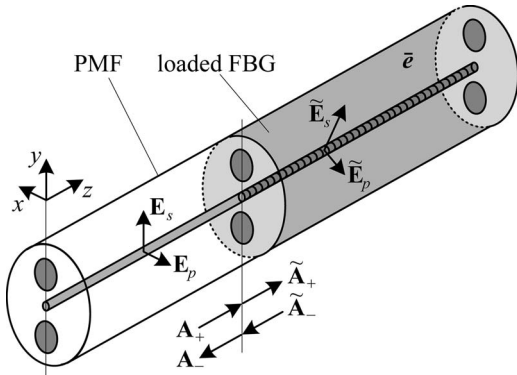

Fig. 1. FBG subject to a mechanical load ($\overline{e}$). The fundamental modes of the FBG change their polarization due to the mechanical perturbation $\overline{\boldsymbol{B}}$.

$$\mathbf{A}_+ = \begin{pmatrix} \widetilde{E}_{p,x} & \widetilde{E}_{s,x} \\ \widetilde{E}_{p,y} & \widetilde{E}_{s,y} \end{pmatrix} \cdot \widetilde{\mathbf{A}}_+ = \underline{Q} \cdot \widetilde{\mathbf{A}}_+. \quad (5)$$

In the fundamental system of the loaded FBG, the coupled-mode equations for polarization cross coupling are decoupled. We can thus treat the problem for each mode separately, by considering the forward–backward coupling induced by the grating structure alone. For this problem, the analytical solution is known, see for example [14]. It is described by the complex reflection coefficient $\rho_i = A_{i-}/A_{i+}$ for mode i, which depends on fixed parameters such as the length of the grating and on variable parameters such as the grating period Λ and the effective refractive index $n_{e,i}$ of the corresponding mode. If we assume that the fixed parameters do not change in an actual measurement situation, the parameters of the analytical solution in the fundamental system of the loaded fiber may be described by $\widetilde{\rho}_i = \rho(\lambda, \Lambda, n_{e,i})$. For the two modes of polarization the two complex reflection coefficients may be summarized in the matrix

$$\widetilde{\boldsymbol{\rho}} = \mathrm{diag}\{\rho(\lambda, \Lambda, n_{e,p}), \rho(\lambda, \Lambda, n_{e,s})\}^T. \quad (6)$$

From these definitions, the amplitudes of the reflected modes in the fundamental system of the loaded FBG are given by

$$\widetilde{\mathbf{A}}_- = \widetilde{\boldsymbol{\rho}} \cdot \widetilde{\mathbf{A}}_+. \quad (7)$$

Equations (5) and (7) then yield

$$\mathbf{A}_- = \underline{Q} \cdot \widetilde{\mathbf{A}}_- = \underline{Q}\widetilde{\boldsymbol{\rho}} \cdot \widetilde{\mathbf{A}}_+ = \underline{Q}\widetilde{\boldsymbol{\rho}}\underline{Q}^{-1} \cdot \mathbf{A}_+ \quad (8)$$

Equation (8) can be interpreted as follows: First the modes of the fiber guiding the light to the FBG are projected onto the fundamental modes of the loaded FBG. In the system of fundamental modes, no polarization coupling takes place, and the conventional reflection coefficients are employed to compute the amplitudes of the reflected fundamental modes. The reflected fundamental modes are then projected back onto the fundamental modes of the fiber. The last step includes the polarization mode coupling and generates the distorted spectra.

To compare the theoretical results with the numerically integrated four-mode coupled-mode theory we compute a wide range of reflection spectra with different parameters of the FBG, all of which show a close agreement with the derived theory. One particular example is given in Fig. 2. The figure shows a simulation of a 3-mm-long FBG with a refractive index modulation amplitude $\Delta n = 1 \times 10^{-4}$ in a PMF with a beat length L_B of 3.5 mm.

The shear strain is set to $e_{xy} = 0.5 \times 10^{-3}$ and $e_{xy} = 1 \times 10^{-3}$, which could arise in an application where the FBG is embedded in a laminated composite, such as in [16], with the difference in the transversal far-field strains e_d^∞ being 6400 μm/m [10] and the fibers' principal axes being oriented at 45° to the coordinate system of the far-field strains and thus transformed following the derivation given in [7]. The illuminating
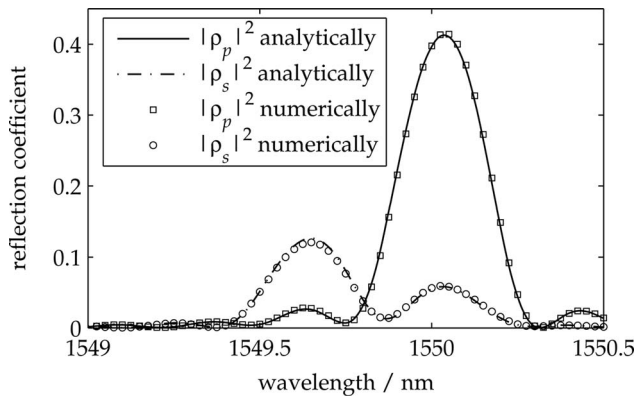
Fig. 2.   Results for a grating with $L_B = 3.5$ mm, $e_{xy} = 1 \times 10^{-3}$, $L = 3$ mm, and $\Delta n = 1 \times 10^{-4}$.

amplitudes are chosen to be $\mathbf{A}_+ = \{1, 1\}^T$. The coupled-mode theory solution closely matches the presented analytical solution, although a small deviation in the peak amplitude may be observed.

The results for a different FBG with a beat length of 4.2 mm and a refractive index modulation amplitude of $\Delta n = 0.5 \times 10^{-4}$ are shown in Fig. 3. Additionally we choose the light source polarization only in the x direction using $\mathbf{A}_+ = \{1, 0\}^T$. The polarization mode coupling can easily be observed in this case as the reflected light shows an intensity in both polarization directions.

Figure 4 illustrates the results of a grating 7 mm in length, with incident illumination set to $\mathbf{A}_+ = \{0.3, 1\}^T$. The beat length is set to 10.6 mm. Again both results are in close agreement.

Summing up, we demonstrated the analytical treatment of shear strain loaded fiber Bragg grating sensors. We derived the required transformation rule from a vectorial wave equation and demonstrated that the results closely match those of the tensorial four-wave coupled-mode approach we previously presented [7]. This analytical treatment may allow the
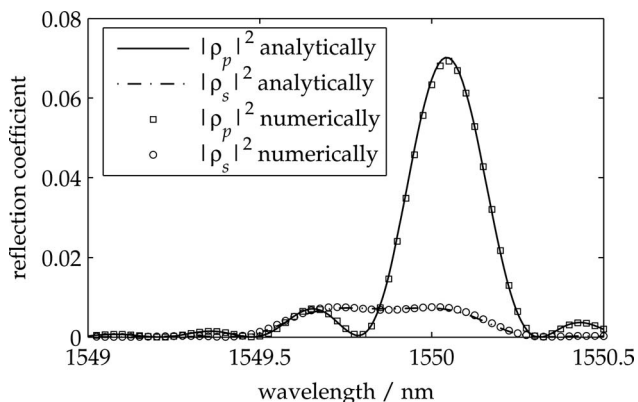

Fig. 3.   Results for a grating with $L_B = 4.2$ mm, $e_{xy} = 1 \times 10^{-3}$, $L = 3$ mm, and $\Delta n = 0.5 \times 10^{-4}$.
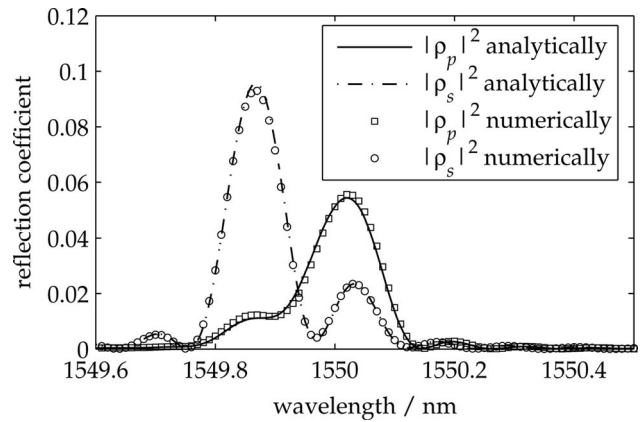

Fig. 4.   Results for a grating with $L_B = 10.6$ mm, $e_{xy} = 0.5 \times 10^{-3}$, $L = 7$ mm, and $\Delta n = 0.3 \times 10^{-4}$.

derivation of algorithms capable of processing the spectral information reflected from shear strain loaded FBGs in such a way that the actual value of the shear strain may be extracted. This would allow for a true reconstruction of the strain tensor at the FBG's sensor position.

References

1. C. Lawrence, D. Nelson, E. Udd, and T. Bennett, Exp. Mech. **39**, 202 (1999).
2. T. Mawatari and D. Nelson, Smart Mater. Struct. **17**, 19 (2008).
3. F. Bosia, P. Giaccari, J. Botsis, M. Facchini, H. Limberger, and R. Salathe, Smart Mater. Struct. **12**, 925 (2003).
4. E. Chehura, C. Ye, S. Staines, S. James, and R. Tatam, Smart Mater. Struct. **13**, 888 (2004).
5. M. Prabhugoud and K. Peters, Smart Mater. Struct. **15**, 550 (2006).
6. E. Udd, W. Schulz, J. Seim, and E. Haugse, in Proc. SPIE **3986**, 254 (2000).
7. M. S. Müller, L. Hoffmann, A. Sandmair, and A. W. Koch, IEEE J. Quantum Electron. **45**, 547 (2009).
8. M. S. Müller, H. El-Khozondar, A. Bernardini, and A. W. Koch, "Transfer matrix approach to four mode coupling in fiber Bragg gratings," IEEE J. Quantum Electron. (to be published).
9. M. S. Müller, T. C. Buck, H. J. El-Khozondar, and A. W. Koch., "Shear-strain influence on fiber Bragg grating measurement systems," J. Lightwave Technol. (to be published).
10. R. J. Van Steenkiste and G. S. Springer, *Strain and Temperature Measurement with Fiber Optic Sensors* (Technomic, 1997).
11. T. Narasimhamutry, *Photoelastic and Electro-Optic Properties of Crystals* (Plenum, 1981).
12. A. Snyder and J. Love, *Optical Waveguide Theory* (Chapman & Hall, 1983).
13. P. Yeh, J. Opt. Soc. Am. **69**, 742 (1979).
14. T. Erdogan, J. Lightwave Technol. **15**, 1277 (1997).
15. M. McCall, J. Lightwave Technol. **18**, 236 (2000).
16. J. A. Guemes and J. M. Menendez, Compos. Sci. Technol. **62**, 959 (2002).